 DOI: 10.1002/masy.201400030

Influence of Counterion on Thermal, Viscoelastic, and Ion Conductive Properties of Phosphonium Ionenes

*Asem I. Abdulahad, Chainika Jangu, Sean T. Hemp, Timothy E. Long**

Summary: Anion metathesis enabled a systematic study focused on the thermal, viscoelastic, and conductivity properties of a 4P,12 phosphonium ionenes with various counterions. Aqueous size exclusion chromatography confirmed the well-defined synthesis of 4P,12-Br from the step-growth polymerization of 1,4-bis(diphenylphosphino) butane and 1,12-dibromododecane at a 1:1 stoichiometric ratio. Subsequent anion-exchange employing a dialysis method exchanged the Br^- counterion to trifluoromethanesulfonate (TfO^-), bis(trifluoromethane) sulfonimide (Tf_2N^-), and tetrafluoroborate (BF_4^-) counterion. ^1H nuclear magnetic resonance spectroscopy of the 4P,12 ionenes showed a distinct upfield chemical shift for methylene protons adjacent to the phosphonium cation after anion-exchange. Thermal characterization using thermogravimetric analysis and differential scanning calorimetry probed the thermal properties of the phosphonium ionenes. Counterion exchange to more bulky and delocalized anions led to improved thermal stabilities and lower glass transition temperatures. Rheological characterization facilitated the generation of time-temperature superposition (TTSp) master curves and pseudo-master curves for each 4P,12 ionene. TTSp revealed two distinct relaxation modes attributed to long-range segmental motion and electrostatic interactions. Anion-exchange resulted in a shift of these two modes of relaxation to higher shear rates. The calculated melt flow activation energy and thermal expansion coefficients were also observed to decrease and increase, respectively. Melt rheological characterization also probed the temperature dependence of the storage and loss moduli and suggested that the counterions have a plasticizing effect on the viscoelasticity of the 4P,12 ionene. Ionic conductivity increased with increasing size of the counterion ($Br^- < BF_4^- < TfO^- < Tf_2N^-$) and demonstrated the viability of these novel materials as potential anion-exchange ionomeric membranes.

Keywords: anion-exchange; conductivity; ionene; phosphonium; structure-property relationship

Introduction

Cationic polyelectrolytes continue to spark intrigue due to their unique physical properties as well as their promise for impacting a variety of emerging technologies. Typical polycations, such as poly(dimethylaminoethyl methacrylate), have positively charged groups within the pendant substituent of the polymer chain, which imparts high charge density and the potential for electrostatic interactions. Due to their inherently high charge density, polycations offer potential in biomedical engineering,[1–4] polymer-based therapeutic formulations,[5–6] battery applications,[7] proton and anion-exchange membranes,[8–9] water and gas purification,[10–12]

Macromolecules and Interfaces Institute, Department of Chemistry, Virginia Tech, Blacksburg, Virginia 24061, USA
Fax: +1 540 231 8517; E-mail: telong@vt.edu

surface modifiers for chromatographic separations and catalytic applications,[13–14] and electroactive actuation.[15]

Ionenes are a unique class of polycations with cationic charges located within the polymer main chain and are typically prepared according to the Menschutkin reaction of a ditertiary alkylamine with a dihaloalkane.[16] Since Gibbs et al. prepared the first ammonium ionenes from halogenated alkyl dimethylamine A-B monomers,[17] this unique class of polyelectrolytes has expanded to include polycations which incorporate imidazolium,[18] pyridinium,[19] and phosphonium[20] charged groups within the polymer backbone. The breadth of difunctional monomers suitable for step-growth polymerization of ionenes has facilitated the study of charge density and polymer architecture for well-defined polymeric materials with precise spacing between cationic charges in both segmented and non-segmented polymers.

Ionenes are typically designated as x,y-ionene, where x and y respectively correspond to the methylene spacer length of the ditertiary amine and dihaloalkane monomers. The study of structure-property relationships of ionenes has primarily focused on ammonium, pyridinium, and imidazolium containing polymers. Wilkes and co-workers demonstrated the dependence of elastomeric behavior of segmented ammonium ionenes on the poly(tetramethylene oxide) soft segment molecular weight.[19,21] Tamami et al. also showed that the solubility and resulting solution behavior of ammonium-based ionenes is variable as a function of alkyl spacer length and counterion.[22] Hemp and co-workers reported structure-property relationships as a function of alkyl spacer length for novel phosphonium-based ionenes where increasing the alkyl spacer length decreased the charge density of phosphonium ionenes and resulted in dramatic differences in viscoelastic response.[20]

Anion metathesis, with inspiration from ionic liquids, has recently become a popular choice for altering the properties of polyelectrolytes. In several literature reports, dramatic changes in polyelectrolyte solubility, solution behavior, conductivity, and viscoelasticity were observed upon exchanging counterions with varying size and/or basicity.[8,23–32] This manuscript details a fundamental study of the structure-property relationship of counterion size and basicity on the properties of a 4P,12-ionene. Aqueous size exclusion chromatography (SEC) confirmed the preparation of a well-defined 4P,12-Br phosphonium ionene using the Menschutkin reaction. Nuclear magnetic resonance spectroscopy was used to confirmed successful anion metathesis to trifluoromethanesulfonate (TfO^-), bis(trifluoromethane) sulfonimide (Tf_2N^-), and tetrafluoroborate (BF_4^-) counterions. Thermal characterization of each 4P,12-ionene indicated a profound influence from the associated counterion, and rheological characterization was used to elucidate the major relaxations within the bulk material. Rheological characterization as a function of temperature suggests the potential for these polymers in high performance applications, and ionic conductivity measurements demonstrate the viability of these novel materialsas potential anion-exchange membranes.

Materials and Methods

Materials

1,4-bis(diphenylphosphino)butane (98%) was purchased from Sigma-Aldrich and recrystallized from chloroform/methanol. 1,12-Dibromododecane (98%) was acquired from Sigma-Aldrich and was distilled under reduced pressure. Sodium trifluoromethanesulfonic acid (98%), lithium bis-(trifluoromethane)sulfonimide, and sodium tetrafluoroboric acid (48 wt% solution in water) were purchased from Sigma-Aldrich and used without further purification. Tetrahydrofuran, hexanes, methanol, hydrochloric acid, and deionized water were obtained from Spectrum Chemicals and used as received.

Synthesis and Anion Metathesis of 4P,12-Br Phosphonium Ionene

Synthesis of the 4P,12 phosphonium ionene with bromide counterions (4P,12-Br) was accomplished by the Menshutkin reaction as previously reported.[20] Briefly, 1,4-bis-(diphenylphosphino) butane (2.5494 g, 5.98 mmol), 1,12-dibromododecane (1.9612 g, 5.98 mmol), and 14.3 mL dimethylformamide were added to a 25-mL, round-bottomed flask with a magnetic stir bar and purged with argon. The resulting heterogeneous solution was heated to 100 °C to obtain a homogeneous solution, and the polymerization was allowed to proceed for 24 h. The resulting polymer solution was diluted with methanol and dialyzed (SpectraPor dialysis membrane; MWCO = 3500 g/mol) against methanol for 3 d. The methanol was removed using rotary evaporation, and the solid polymer was obtained after drying at 80 °C for 24 h *in vacuo*.

Anion-exchange from bromide counterions to respective counterions of tetrafluoroborate (BF_4^-), trifluoromethanesulfonate (TfO^-), and bis(trifluoromethane) sulfonimide (Tf_2N^-) were each accomplished using a dialysis method. The 4P,12-Br polymer was dissolved in acetone at 5 wt% and 5 molar equivalents of the counterion salt was separately dissolved in acetone. The polymer solution was added to the counterion salt solution dropwise and this mixture was dialyzed against pure acetone. Over a 3 d period, the dialysis solvent was changed and 20 mL of the 5 molar equivalents counterion salt solution was added to the dialysis tubing every 12 h. Subsequently, the anion-exchanged polymer solutions were dialyzed against pure acetone for an additional 3 d (changing the dialysis solvent every 12 h) to remove any excess, non-interacting counterions.

Analytical Methods

Aqueous size exclusion chromatography (SEC) was performed using a mixed mobile phase consisting of 54/23/23 (v/v/v%) water/methanol/acetic acid with 0.1 M sodium acetate, two Waters ultrahydrogel linear columns, and one Waters ultrahydrogel 250 column. The instrumentation used included a Waters 1515 isocratic solvent delivery pump, Waters 717plus autosampler, Waters 2414 refractive index detector, and a Wyatt MiniDawn light scattering detector, which collectively enabled the determination of absolute molecular weight. In order to determine absolute molecular weights, the refractive index dependence on concentration (dn/dc) was obtained using a Wyatt Opti-lab T-rEX refractometer ($\lambda = 658$ nm). Thermogravimetric analysis (TGA) employed a TA Instruments TGA Q50 and the temperature at 5% weight loss was determined by heating from 100 °C to 600 °C at a heating rate of 10 °C/min after an isothermal drying step maintaining a furnace temperature of 100 °C for 60 min. Differential scanning calorimetry (DSC) was accomplished using a TA Instruments DSC Q1000 under nitrogen atmosphere with a heat/cool/heat cycle performed at 10 °C/min. ^{1}H nuclear magnetic resonance (NMR) spectra were obtained in CD_2Cl_2 at 23 °C using a Varian Unity 400 spectrometer.

Rheological Characterization

Polymer melt rheological characterization was performed under inert atmosphere using a TA Instruments DHR-2 rheometer equipped with an 8 mm parallel plate geometry. Strain-sweep experiments (0.004 - 4.0% oscillatory strain at 1 Hz) were used to first determine the linear viscoelastic region for each anion-exchanged phosphonium ionene. Frequency sweep experiments were performed for each sample at an oscillatory strain of 1.25% using 10 °C temperature steps and an angular frequency range from 0.1 - 100 rad/s. The resulting storage and loss moduli for each polymer were shifted to build master and pseudomaster curves using the TA Instruments provided TRIOS software package. Master curves based on shifting and overlapping of the storage and loss moduli generated horizontal shift factors (a_T). Pseudomaster curves were obtained by fitting only the loss modulus data. According to Arrhenius analysis in the

terminal flow region, the pseudomaster curves provided suitable shift factors for the determination of melt flow activation energies. Figures confirming adherence of master curve shift factors to the Williams-Landel-Ferry equation are displayed in the Supplemental information for Arrhenius analysis to determine values of melt flow activation energy for each ionene. The dependence of storage and loss moduli on temperature was actively assessed with an 8 mm parallel plate geometry using a temperature ramp within the linear viscoelastic region for each phosphonium ionene at 0.5 °C/min, 1.25% oscillatory strain, and an angular frequency of 1.0 rad/s.

Impedance Spectroscopy

Electrochemical impedance spectroscopy (EIS) was performed using an Autloab PGSTAT 302N potentiostat and a four-point electrode sample cell purchased from BekkTeck, Inc. An applied alternating sine-wave potential was applied at 0.2 V with frequencies ranging from 0.1 Hz to 1 MHz. The temperature and relative humidity (RH) was controlled using an ESPEC BTL- 433 environmental chamber, which controlled the temperature to ± 0.1 °C and 10% RH to ± 0.1%. An alternating current was applied to the outer electrodes and the real impedance or resistance, R, was measured between the two inner reference electrodes. The resistance was determined from a high x-intercept of the semicircle regression of the Nyquist plot. The ionic conductivity was determined by $\sigma = L/AR$, where L and A are the distance between the two inner electrodes and the cross-sectional area of the polymer film, respectively. The cross-sectional area is defined as $A = Wl$, where W is the film width and l is the film thickness. Samples were allowed to equilibrate for 1 h at each measurement condition followed by at least five measurements at that condition. The values reported are an average of these steady-state measurements. Polymer films were prepared using a solution cast method. Each anion-exchanged phosphonium ionene was dissolved at 20 wt% in acetone and cast onto silicon-coated Mylar® film. Each solution casted film was allowed to dry at room temperature for 5 d and subsequently annealed *in vacuo* for an additional 3 d.

Results and Discussion

Polymerization of 4P,12-Br Phosphonium Ionene

Synthesis of phosphonium ionenes was accomplished using the Menschutkin reaction between a ditertiary phosphine and dibromoalkane to yield a cationic phosphonium ionene. Recently published literature from our research group details the preparation of phosphonium ionenes with various alkylene spacer lengths. Similar to ammonium ionenes, phosphonium ionenes were labeled xP,y, where x and y respectively denote the alkyl spacer length in the ditertiary phosphine and dihaloalkane.[20]

Scheme 1A depicts the reaction of 1,4-bis(diphenylphosphino) butane with 1,12-dibromododecane to produce a 4P,12 phosphonium ionene with bromide counterions. The polymerization was accomplished in a one-step synthesis where 1:1 molar equivalents of the ditertiary phosphine and dibromoalkane were added to a 25-mL, round-bottomed flask and reacted in N,N-dimethylformamide for 24 h at 100 °C. Aqueous size exclusion chromatography (SEC) employed a ternary mobile phase mixture of water/methanol/acetic acid (54/23/23 (v/v/v%)) and 0.1 M sodium acetate, which effectively screened electrostatic interactions to enable absolute molecular weight determination using an in-line multi-angle laser light scattering (MALLS) detector. Figure 1 shows the experimentally determined number-average and weight-average molecular weights and the SEC chromatogram for the 4P,12-Br ionene prior to anion metathesis.

Chemical Characterization of Anion-Exchanged 4P,12 Ionenes

Scheme 1B shows a general reaction scheme for the anion metathesis displacing the bromide counterions with tetrafluoroborate (BF_4^-),

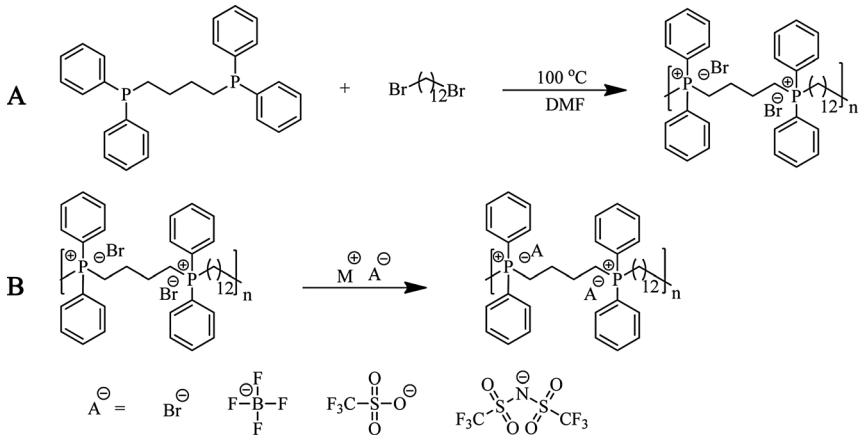

Scheme 1.
Polymerization of 1,4-bis(diphenylphosphino) butane and 1,12-dibromododecae (**A**). Generalized scheme for the anion metathesis of the bromide anion to prepare the 4P,12-BF_4, 4P,12-TfO, 4P,12-Tf_2N ionenes (**B**).

trifluoromethansulfonate (TfO^-), and bis-(trifluoromethane) sulfonimide (Tf_2N^-). The resulting anion-exchanged phosphonium ionenes were characterized using ^{1}H NMR spectroscopy. The corresponding NMR spectra are displayed in Figure 2, and the spectra interestingly show that anion metathesis from bromide to bulkier fluorinated counterions resulted in an upfield chemical shift for methylene protons adjacent to phosphonium cations. Anion-exchange to Tf_2N^- shows the most pronounced upfield shift as compared to the 4P,12-Br precursor. Two distinct chemical shifts exist for the phosphonium ionene precursor at 3.57 and 3.14 ppm, while the 4P,12-Tf_2N derivative shows a bimodal peak near 2.75 ppm. ^{1}H NMR spectroscopy confirmed complete anion metathesis due to the complete shift of the two methylene peaks.

Influence of Thermal Properties on Counterion

Thermogravimetric analysis (TGA) and differential scanning calorimetry (DSC) indicated that the counterion displayed a strong influence on the thermal properties

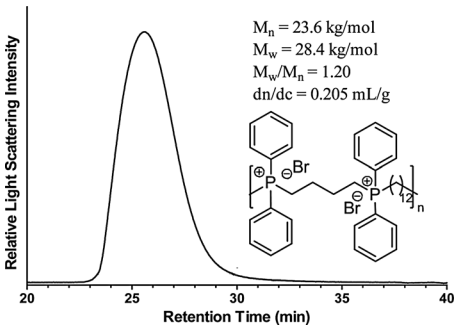

Figure 1.
Aqueous SEC chromatogram of the 4P,12-Br phosphonium ionene.

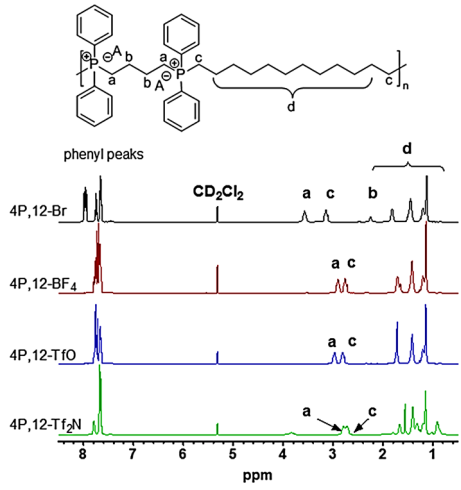

Figure 2.
^{1}H NMR spectra for 4P,12-Br and anion-exchanged analogs: 4P,12-BF4, 4P,12-TfO, and 4P,12-Tf2N.

of 4P,12 ionenes. The DSC curves displayed in Figure 3A show a dramatic dependence on the size of the associated counterion with the glass transition temperature (T_g), decreasing with increasing size of the associated counterion as follows: Tf_2N^-< TfO^-< BF_4^-< Br^-. The glass transition temperatures for Br^-, BF_4^-, TfO^-, and Tf_2N^- containing 4P,12 ionenes as determined by DSC are listed in Table 1. The T_g values indicate that anion metathesis result in an overall change in T_g of approximately 100 °C and suggest that increasing the size of the associated counterion facilitates long range segmental motion. The observed trend in glass transition temperature is in good agreement with previously published literature.[33–37] In one representative study, Hunley et al. also showed that the T_g of protonated poly(dimethylaminoethyl methacrylate) was profoundly influenced by the presence of bulkier fluorinated counterions.[33]

The TGA traces shown in Figure 3B also corroborate previous literature reports on ammonium or imidazolium ionenes, which indicate that the thermal stability is dependent upon the basicity of the associated counterion.[22,38] Similarly, 4P,12 ionenes showed an improvement in thermal degradation beyond 400 °C for 4P,12-TfO and 4P,12-Tf_2N materials. Recent publications from our research group comparing ammonium and phosphonium polymerized ionic liquids present phosphonium-based polymerized ionic liquids as more resistant to degradation through a reverse Menschutkin reaction leading to enhanced thermal stability.[22,39–40] The temperature at 5% weight loss ($T_{d,5\%}$; summarized in Table 1) was enhanced nearly 100 °C upon anion metathesis from bromide to Tf_2N^- counterions, which confirms that counterion exchange heavily influences the thermal properties of ionenes.

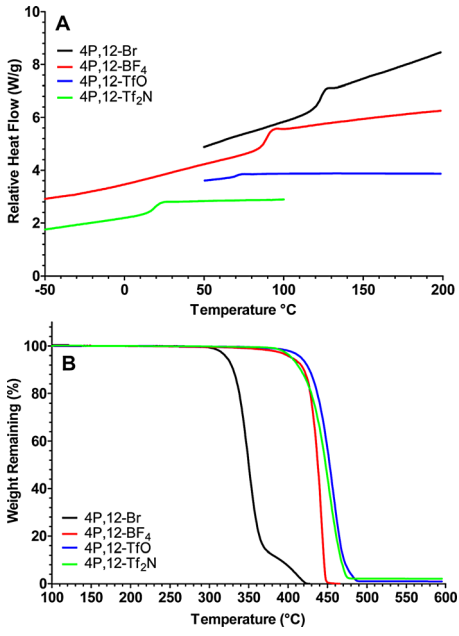

Figure 3.
DSC traces (A) and TGA traces (B) for for 4P,12-ionenes with different counterions.

Table 1.
Glass transition temperatures and degradation temperatures for 4P,12-ionenes with different counterions as determined by DSC and TGA, respectively.

Ionene	T_g (°C)	$T_{d,5\%}$ (°C)
4P,12-Br	123	320
4P,12-BF_4	90	399
4P,12-TfO	71	415
4P,12-Tf_2N	19	404

Influence of Phosphonium Ionene Counterion on Viscoelasticity

The structure-property relationship dependence of phosphonium ionenes on alkylene spacer length between the ditertiary phosphine and dibromide monomers was recently examined in order to discern the impact of charge density on thermal and viscoelastic properties of these polycations.[20] The unique thermal properties of phosphonium ionenes, including relatively low T_g's and high degradation temperatures, present a unique opportunity to probe the influence of electrostatic interactions on their melt flow dynamics through melt rheological characterization. The influence of counterion on the viscoelasticity of phosphonium ionenes at constant charge density was explored within the linear viscoelastic region by application of the

principles of time-temperature superposition (TTSp). At a constant oscillatory strain of 1.25% within the linear viscoelastic regime, frequency sweep experiments were performed in 10 °C temperature steps. Temperature ramp experiments were also performed within the linear viscoelastic region using a constant oscillatory strain of 1.25% and constant oscillation frequency of 1.00 rad/s.

Figure 4A displays master curves for both the storage and loss moduli (respectively denoted as G' and G") for all anion-exchanged phosphonium ionenes. Shift factors for producing TTSp master curves for each anion-exchanged phosphonium ionene were determined using a reference temperature (T_r) of 130 °C. Superimposition of the experimental data shows acceptable overlap over an angular frequency range spanning 8-10 decades for both G' and G" master curves for all anion-exchanged phosphonium ionenes confirming that TTSp principles are upheld. The storage and loss moduli master curves also depict two distinct relaxation phenomena. The onset of long range segmental motion of polymer chains is observed at shorter relaxation time-scales (i.e. high oscillation frequency) and is a phenomenon characteristic to viscoelastic materials.[37,41] A second mode of relaxation appears at low oscillation frequencies before the onset of terminal flow. In corroboration with previously published literature from Nakamura and co-workers,[34,36,42] this mode of relaxation is attributed to electrostatic interactions found in polycations. Anion metathesis of the 4P,12 phosphonium ionene had a profound impact on the viscoelastic behavior of the resulting materials with relaxation modes representative of both electrostatic interactions as well as long range segmental motion of polymer chains occurring at longer relaxation time scales, where the size and basicity of the counterion respectively influence the long range segmental motion and the electrostatic interactions of the polymer.

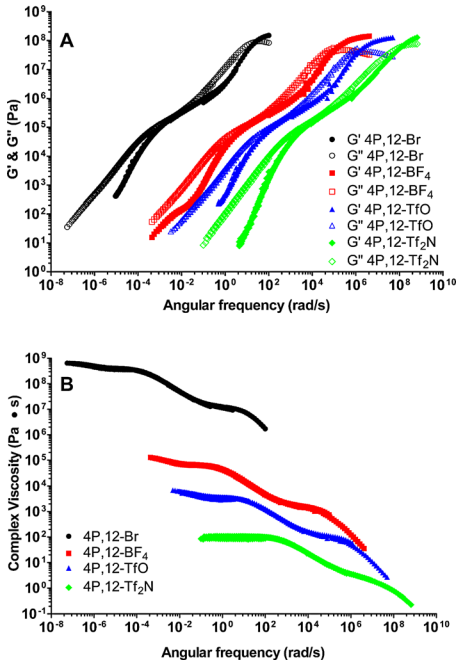

Figure 4.
Master curves of storage and loss moduli (A) and pseudo-master curves of complex viscosity (B) for 4P,12-ionenes with varying counterions ($T_r = 130$ °C).

Figure 4B displays pseudo-master curves for the anion-exchanged 4P,12 phosphonium ionenes as a plot of the complex viscosity versus oscillation frequency. The shift factors used to generate these pseudo-master curves were determined from only the loss moduli of the anion-exchanged 4P,12 ionenes. Arrhenius analysis of the shift factors ($T_r = 130$ °C) enabled determination of the melt flow activation energy (summarized in Table 2). The melt flow activation energy also shows a strong dependence upon the size of the counterion. Anion metathesis leads to a wide range of values for melt flow activation energy between 69 and 171 kJ/mol and increases with decreasing counterion size (Tf_2N^- > TfO^- > BF_4^- > Br^-).

The dependence of the shift factors on temperature for all anion-exchanged 4P,12 ionenes showed excellent adherence to the Williams-Landel-Ferry (WLF) equation. The WLF equation (equation 1 below) was used to determine the material specific C_1 and C_2 constants, which are dependent upon the reference temperature employed

Table 2.
Williams-Landel-Ferry (WLF) parameters, fractional free volumes, thermal expansion coefficients, and melt flow activation energies for 4P,12-ionenes with various counterions.

Ionene	C_1	C_2 (K)	C_1^g	C_2^g (K)	f_g	α_f (10^{-4} K^{-1})	E_a (kJ/mol)
4P,12-Br	9.79	57.1	11.2	50.1	0.039	7.77	171
4P,12-BF_4	6.03	92.0	10.7	52.0	0.041	7.82	120
4P,12-TfO	4.96	112	10.5	53.1	0.041	7.81	97.0
4P,12-Tf_2N	2.78	155	9.76	44.2	0.044	10.1	69.0

for generating TTSp master curves. The C_1 and C_2 constants, were normalized by T_g values for the respective anion-exchanged 4P,12 ionenes using the following relationships (equations 2 and 3 below). Comparison of C_1^g and C_2^g values obtained for the anion-exchanged 4P,12 ionenes show good correlation to literature values obtained for charged polymers as well as for neutral polymers.[29,37] C_1^g and C_2^g constants were subsequently employed for the calculation of fractional free volume as well as thermal expansion coefficients for all anion-exchanged 4P,12 ionenes using equations 3 and 4, respectively. Based upon literature precedence, a value of 1 was assumed for B.[40,43] The fractional free volume, thermal expansion coefficients, as well as material specific WLF constants are summarized in Table 2.

$$\log(a_T) = \frac{-C_1(T - T_r)}{C2 + (T - T_r)} \quad (1)$$

$$C_1^g = \frac{C_1 C_2}{C_2 + (T_g - T_r)} \quad (2)$$

$$C_2^g = C_2(T_g - T_r) \quad (3)$$

$$f_g = \frac{B}{2.303 C_1^g} \quad (4)$$

$$a_f = \frac{B}{2.303 C_1^g C_2^g} \quad (5)$$

Melt Flow Rheology of 4P,12 Ionenes

Temperature ramp rheological experiments were performed in order to ascertain the temperature dependence as a function of counterion. To ensure assessment of each phosphonium ionene within the melt state, rheological measurements were performed within a temperature range that began slightly above T_g and within the viscoelastic regime at low oscillation strain rate and strain % (1.00 rad/s and 1.25% respectively) using an 8mm parallel plate geometry. Figure 5 shows the storage and loss moduli (G' and G" respectively) as a function of temperature. The loss modulus remains greater than the storage modulus for each 4P,12ionene, and the viscosity decreases, as expected, with increasing temperature until the onset of terminal flow. Overall, the counterion has a significant impact on the temperature dependent viscoelasticity. The storage and loss moduli both decrease dramatically with anion-exchange from bromide to the bulkier fluorinated counterions, and the magnitude of the loss and storage moduli show the following trend 4P,12-Br > 4P,12-BF_4> 4P,12-TfO > 4P,12-Tf_2N. The impact of counterion size on viscoelasticity suggests that the counterion has a plasticizing effect on the bulk properties of the polymeric materials.

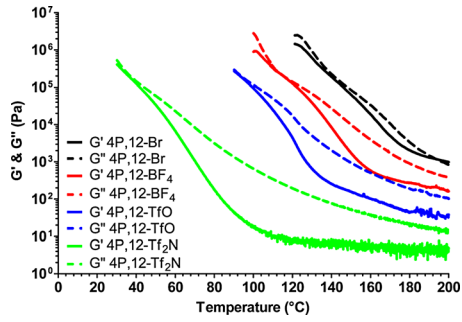

Figure 5.
Temperature ramp rheology showing the dependence of storage and loss moduli (G' and G") on temperature.

Ionic Conductivity

The temperature-dependent ionic conductivity of 4P,12 ionenes with different counterions are shown in Figure 6. Experimental constraints limited the sample selection to polymers with T_g's below 150 °C, which was the maximum temperature for the environmental chamber. Similar to previous literature reports,[28–29,33,36] the exchange from the more hydrophilic bromide anion to relatively more hydrophobic, bulkier fluorine-containing anions such as BF_4^-, TfO^-, or Tf_2N^-, increased the relative hydrophobicity and resulted in water-insoluble polymers. Anion-exchange from the Br^- counterion to BF_4^-, TfO^- or Tf_2N^- reduced the T_g significantly and increased the thermal stability due to reduced anion basicity as well as the increased size of the counterion. The ionic conductivity increased over an order-of-magnitude when the counterion changed from TfO^- to Tf_2N^-. The 4P,12-Tf_2N polymers have higher ionic conductivities relative to 4P,12-TfO^- polymers. The higher ionic conductivity was attributed to lower T_g(as observed from DSC and melt rheological characterization displayed in Figure 3A and Figure 5, respectively) of the larger Tf_2N^- anion, which enhances segmental relaxation of the polymer chains and improves ion mobility within the polymer. The ionic conductivity results show that the glass transition temperature (T_g) is a dominant, but not exclusive, parameter in determining ion transport.

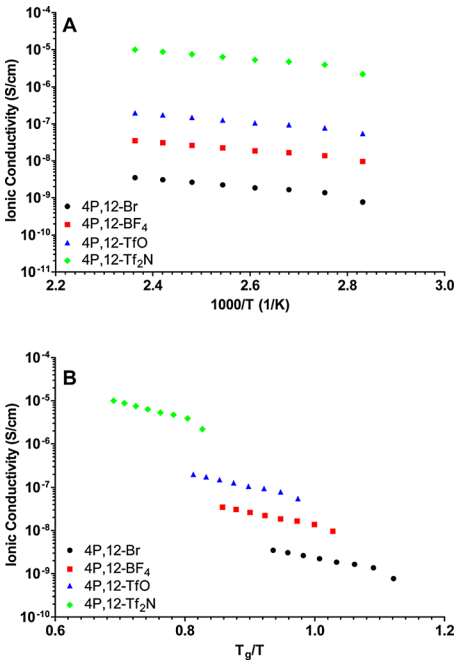

Figure 6.
Ionic conductivity for 4P,12 ionenes with various counterions as a function of (a) 1000/T and (b) Tg/T for polymers with various counterions.

Conclusion

4P,12-Br phosphonium ionenes were prepared by step-growth polymerization employing the Menschutkin reaction. Subsequent anion metathesis was used to exchange the bromide counterion to prepare 4P,12-Tf_2N, 4P,12-TfO, and 4P,12-BF_4. A comparison of nuclear magnetic resonance spectroscopy showed characteristic upfield chemical shifts resulting from anion-exchange to the bulkier, fluorinated anions. The size and basicity of the counterion also had a profound impact on the thermal and viscoelastic properties of the resulting materials. Anion metathesis to larger, weaker anions led to dramatically reduced glass transition temperatures while the degradation temperature at 5% weight loss was enhanced from 300 °C to above 400 °C. Time-temperature superposition (TTSp) also showed a profound influence of rheological properties on the associated counterion. Two modes of relaxation corresponding to the onset of long-range segmental motion (T_g) and electrostatic interactions were observed, and anion-exchange led to a shift in these distinct relaxation modes to longer time scales. This observed shift was more pronounced for the bulkier Tf_2N^- and TfO^- counterion containing materials. Melt rheological characterization provided the impact of anion-exchange on the dependence of viscoelastic moduli on temperature. Overall, it was observed that that counterions behave as plasticizers to effectively enhance

polymer chain mobility in the melt; this is also evident from the reduction in glass transition temperature observed from DSC analysis. Ionic conductivity was also greatly influenced by the size and basicity of the associated counterion. The ionic conductivity increased over an order of magnitude when counterion changed from TfO^- to Tf_2N^-. The 4P,12-Tf_2N specimen had higher ionic conductivity relative to 4P,12-TfO polymers. The higher ionic conductivity was attributed to an enhanced plasticization effect of the larger Tf_2N^- anion that enhances segmental relaxation of the polymer chains and improves ion mobility within the bulk material.

Acknowledgments: This material is based upon work supported in part by the U.S. Army Research Laboratory and the U.S. Army Research Office under the Army Materials Center of Excellence Program, contract W911NF-06-2-0014. We also acknowledge The Brown Foundation and the Virginia Tech College of Science for additional financial support as well as the Virginia Tech Institute for Critical Technology and Applied Science (ICTAS) for facility support.

[1] P. Coimbra, P. Ferreira, H. C. de Sousa, P. Batista, M. A. Rodrigues, I. J. Corriea, M. H. Gil, *Int. J. Biol. Macromol.* **2011**, *48*, 112.
[2] D. Raghothaman, M. F. Leong, Z. Yang, K. C. J. Toh, T. C. A. Lim, C. A. A. Wan, H. L. Eng, *J. Tissue Eng. Regener. Med.* **2012**, *6*, 69.
[3] B. C. U. Tai, S. Gao, C. Du, A. C. A. Wan, J. Y. Ying, *Tissue Eng., Part A* **2008**, *14*, 767.
[4] E. K. F. Yim, I. C. Liao, K. W. Leong, *Tissue Eng.* **2007**, *13*, 423.
[5] T. A. Al-Hilal, F. Alam, Y. Byun, *Adv. Drug Deliv. Rev.* **2013**, *65*, 845.
[6] J. Panyam, V. Labhasetwar, *Adv. Drug Deliv. Rev.* **2012**, *64*, 61.
[7] J. L. Lutkenhaus, P. T. Hammond, *Soft Matter.* **2007**, *3*, 804.
[8] K. J. Noonan, K. M. Hugar, H. At. Kostalik, E. B. Lobkovsky, H. D. Abruna, G. W. Coates, *J. Am. Chem. Soc.* **2012**, *134*, 18161.
[9] M. Hickner, H. Ghassemi, Y. Kim, B. Einsla, J. McGrath, *Chem. Rev.* **2004**, *104*, 4587.
[10] Y. Wan, H. Wu, A. Yu, D. Wen, *Biomacromolecules* **2006**, *7*, 1362.
[11] A. Saxena, A. Kumar, V. Shahi, *J. Colloid Interface Sci.* **2006**, *303*, 484.
[12] K. C. Trevor, E. B. Jason, L. L. Andrew, L. G. Douglas, D. N. Richard, *J. Membr. Sci.* **2010**, 359.
[13] R. C. Bazito, F. L. Cassio, F. H. Quina, *Macromol. Symp.* **2005**, *229*, 197.
[14] M. F. Munhoz, F. H. Quina, *Macromol. Symp.* **2006**, *245*, 232.
[15] V. Finkenstadt, *App. Microbiol. Biotechnol.* **2005**, *67*, 735.
[16] S. R. Williams, T. E. Long, *Prog. Polym. Sci.* **2009**, *34*, 762.
[17] C. F. Gibbs, C. S. Marvel, *J. Am. Chem. Soc.* **1934**, *56*, 725.
[18] S. R. Williams, D. Salas-de la Cruz, K. I. Winey, T. E. Long, *Polymer* **2010**, *51*, 1252.
[19] D. Feng, G. Wilkes, B. Lee, J. McGrath, *Polymer* **1992**.
[20] S. T. Hemp, M. S. Zhang, M. Tamami, T. E. Long, *Polym. Chem.* **2013**, *4*, 3582.
[21] D. Feng, L. N. Venkateshwaran, G. L. Wilkes, M. L. Charles, E. S. John, *J. Appl. Polym. Sci.* **1989**, 38.
[22] M. Tamami, D. Salas-de la Cruz, K. I. Winey, T. E. Long, *Macromol. Chem. Phys.* **2012**, *213*, 965.
[23] P. M. Carrasco, A. R. de Luzuriaga, M. Constantinou, P. Georgopanos, S. Rangou, A. Avgeropoulos, N. E. Zafeiropoulos, H. J. Grande, G. Cabanero, D. Mecerreyes, I. Garcia, *Macromolecules* **2011**, *44*, 4936.
[24] T. Sata, S. I. Emori, K. Matsusaki, *J. Polym. Sci., Part B: Polym. Phys.* **1999**, *37*, 793.
[25] T. Sata, K. Matsusaki, *J. Polym. Sci. Pol. Chem.* **1996**, *34*, 2123.
[26] T. Sata, S. Nojima, K. Matsusaki, *Polymer* **1999**, *40*, 7243.
[27] T. Sata, M. Tsujimoto, T. Yamaguchi, K. Matsusaki, *J. Membr. Sci.* **1996**, *112*, 161.
[28] T. Sata, Y. Yamane, K. Matsusaki, *J. Polym. Sci. Pol. Chem.* **1998**, *36*, 49.
[29] Y. S. Ye, Y. A. Elabd, *Polymer* **2011**, *52*, 1309.
[30] R. Marcilla, J. A. Blazquez, R. Fernandez, H. Grande, J. A. Pomposo, D. Mecerreyes, *Macromol. Chem. Phys.* **2005**, *206*, 299.
[31] R. Marcilla, J. A. Blazquez, J. Rodriguez, J. A. Pomposo, D. Mecerreyes, *J. Polym. Sci. Pol. Chem.* **2004**, *42*, 208.
[32] R. Marcilla, M. Sanchez-Paniagua, B. Lopez-Ruiz, E. Lopez-Cabarcos, E. Ochoteco, H. Grande, D. Mecerreyes, *J. Polym. Sci. Pol. Chem.* **2006**, *44*, 3958.
[33] M. T. Hunley, J. P. England, T. E. Long, *Macromolecules* **2010**, *43*, 9998.
[34] K. Nakamura, K. Fukao, T. Inoue, *Macromolecules* **2012**, *45*, 3850.
[35] G. Godeau, L. Navailles, F. Nallet, X. R. Lin, T. J. McIntosh, M. W. Grinstaff, *Macromolecules* **2012**, *45*, 2509.
[36] K. Nakamura, T. Saiwaki, K. Fukao, T. Inoue, *Macromolecules* **2011**, *44*, 7719.

[37] Q. Wu, R. A. Weiss, *Polymer* **2007**, *48*, 7558.
[38] M. D. Green, D. Salas-de la Cruz, Y. S. Ye, J. M. Layman, Y. A. Elabd, K. I. Winey, T. E. Long, *Macromol. Chem. Phys.* **2011**, *212*, 2522.
[39] S. T. Hemp, M. Zhang, M. H. Allen, S. Cheng, R. B. Moore, T. E. Long, *Macromol. Chem. Phys.* **2013**, *214*, 2099.
[40] N. K. Tierney, R. A. Register, *Macromolecules* **2003**, *36*, 1170.
[41] V. Jovanovski, R. Marcilla, D. Mecerreyes, *Macromol. Rapid Commun.* **2010**, *31*, 1646.
[42] K. Nakamura, K. Fukao, *Macromolecules* **2011**, *44*, 3053.
[43] Y. Ikeda, H. Masui, Y. Matoba, *J. Appl. Polym. Sci.* **2005**, *95*, 178.

